Figure S1

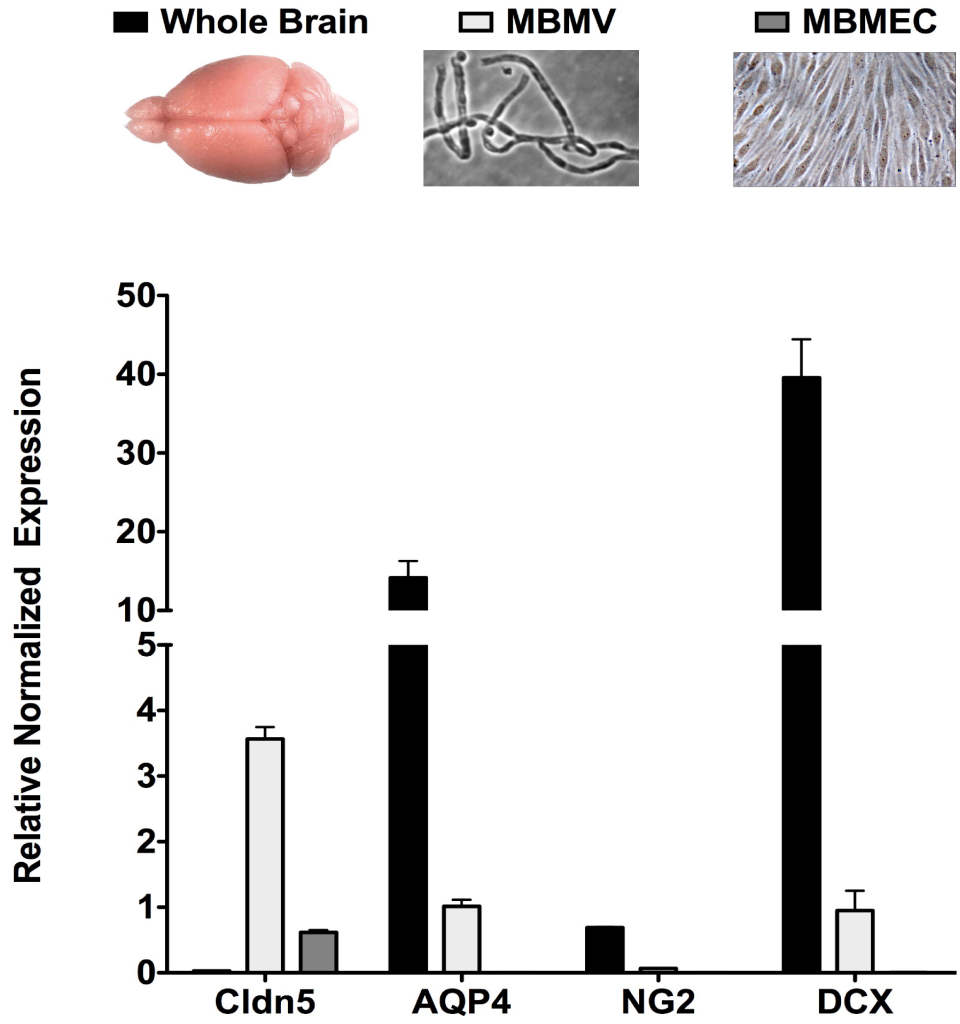

Figure S1 Purity analysis of brain microvessels and endothelial cells

Mouse brain microvessels (MBMV) and endothelial cells (MBMECs) were subjected to qRT-PCR analysis to evaluate the level of contamination by astrocytes, pericytes, and neurons in comparison to whole brain lysates. With aquaporin-4 (AQP4) as a marker for astrocytes, MBMECs showed absence of astrocytes whereas MBMV showed minimal contamination. This was also true for the pericyte (NG2) and the neuronal (DCX) markers where MBMV showed some contamination but MBMECs were entirely free of these cell types. Cldn5 showed enrichment of endothelial cells in the MBMV and MBMECs compared to whole brain. Expression normalization was performed with RPLP0 as a housekeeping gene. (Representative of n=2 using 4-5 brains in each preparation).

Figure S2

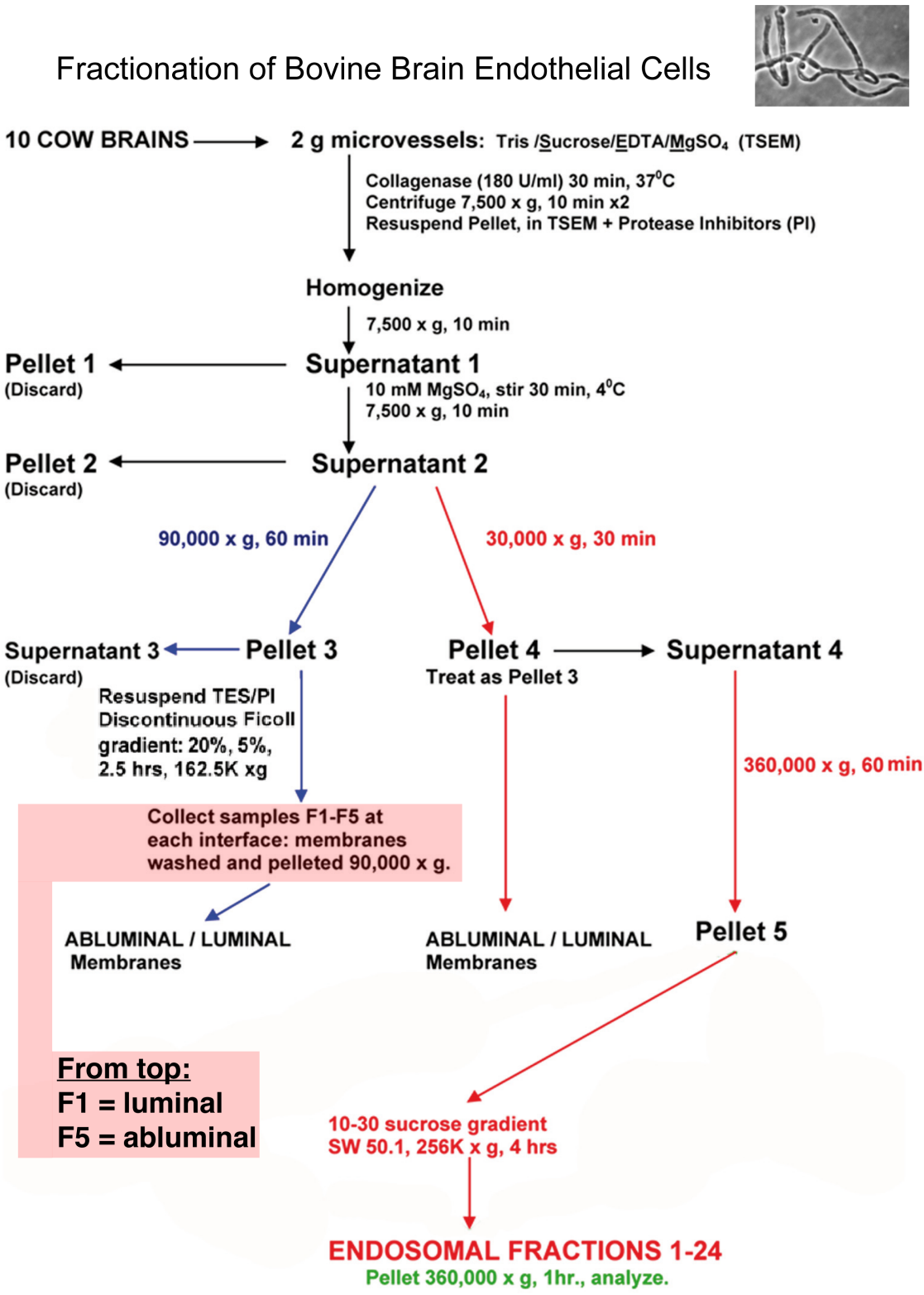

Figure S2 Flow diagram showing fractionation of bovine brain endothelial cells

Figure S3

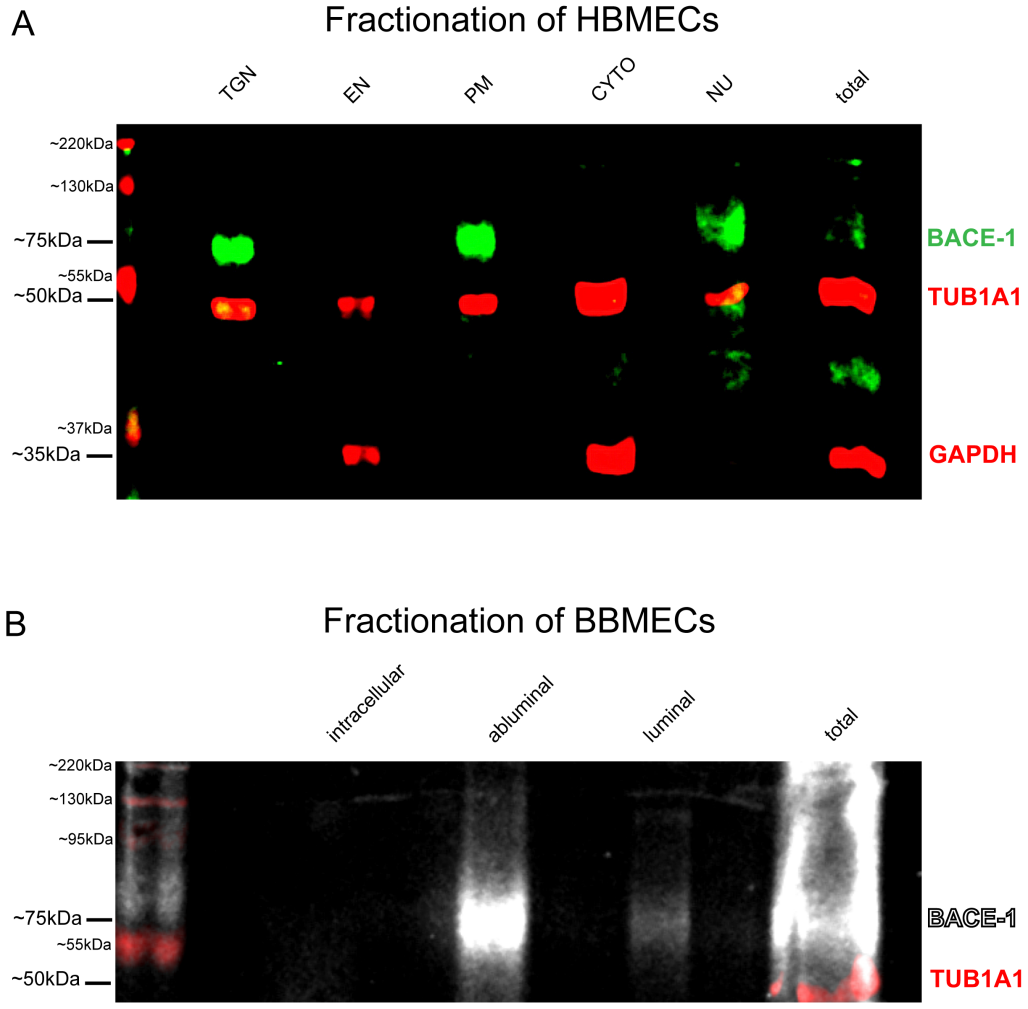

Figure S3 Multi-color Western blots showing BACE-1 in bovine and human brain endothelial fractions

A) Two-channel image (Odyssey, Li-COR) showing BACE-1 in green and TUB1A1, GAPDH in red. The blot shows specificity of BACE-1 and enrichment of BACE-1 in plasma membrane (PM) and Golgi (TGN) fractions with minimal enrichment in the cytoplasmic as well as endosomal (EN) fractions. GAPDH was present primarily in the cytoplasmic (CYTO) fraction, which also partly contaminated the EN fraction. The nuclear (NU) fraction shows contamination with other fractions potentially owing to incomplete homogenization. B) Specificity and predominant abluminal localization of BACE-1 (in white) is detectable in bovine endothelial membrane fractions. The bovine endothelial intracellular vesicle fraction similar to the EN fraction of HBMEC had minimal BACE-1 content. TUB1A1 in red is present only in the starting total microvessel sample. Loading was confirmed with ponceau S staining. Samples in A and B figures are from a different set than presented in the corresponding main figures 4D and 3D respectively.

Figure S4

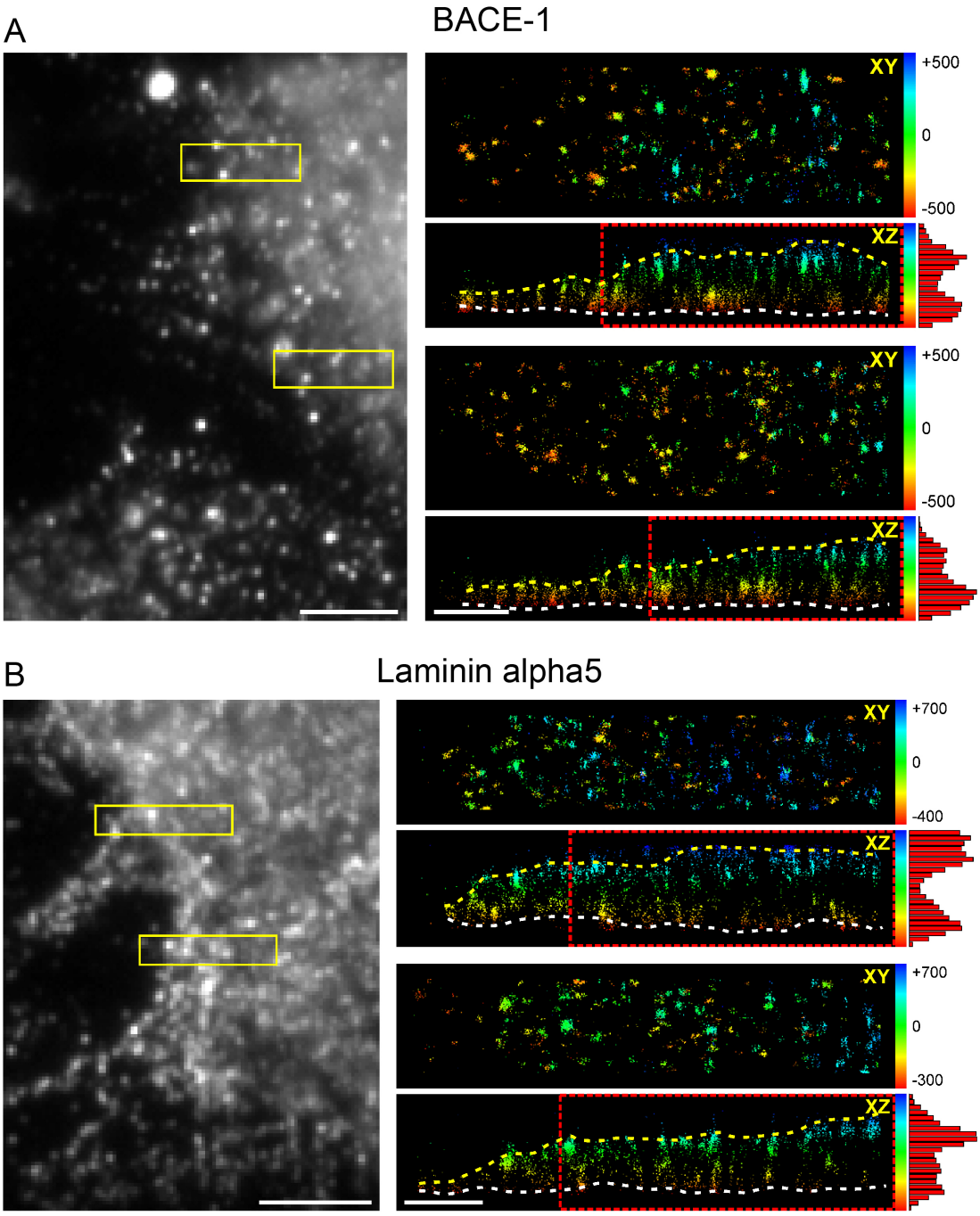

Figure S4 3D dSTORM localization of BACE-1 in HBMECs

A) 3D dSTORM-imaging of Alexa-Fluor 647 labeled BACE-1. Diffraction limited widefield fluorescence image of an HBMEC is shown in the overview (left image). BACE-1 is preferentially located close to the plasma membrane as shown by the cross-sections of small insets (XZ). The yellow and white dotted lines mark the apical (top) and basal (bottom) plasma membranes respectively. Insets are color-coded according to the relative z-position in nm, as indicated by the values. Scale bar 5 and 1µm (overview and insets, respectively). **B)** 3D dSTORM-imaging of Alexa-Fluor

647 labeled laminin α5 for indirect membrane visualization. Diffraction limited widefield fluorescence image shows an overview of the staining (left image). The cross-sections of small insets (XZ) show similar axial distributions to the BACE-1 distribution confirming membrane localization of BACE-1. Numbers indicate the relative z-position in nm. Scale bar 5 and 1μm (overview and insets, respectively). Histograms on the right show quantifications of axial BACE1 localization. HBMECs in this figure are from a different donor than used in corresponding main figure 4. The cell shown in figure A is different from that of figure B but the field is very similar in both cells.

Figure S5

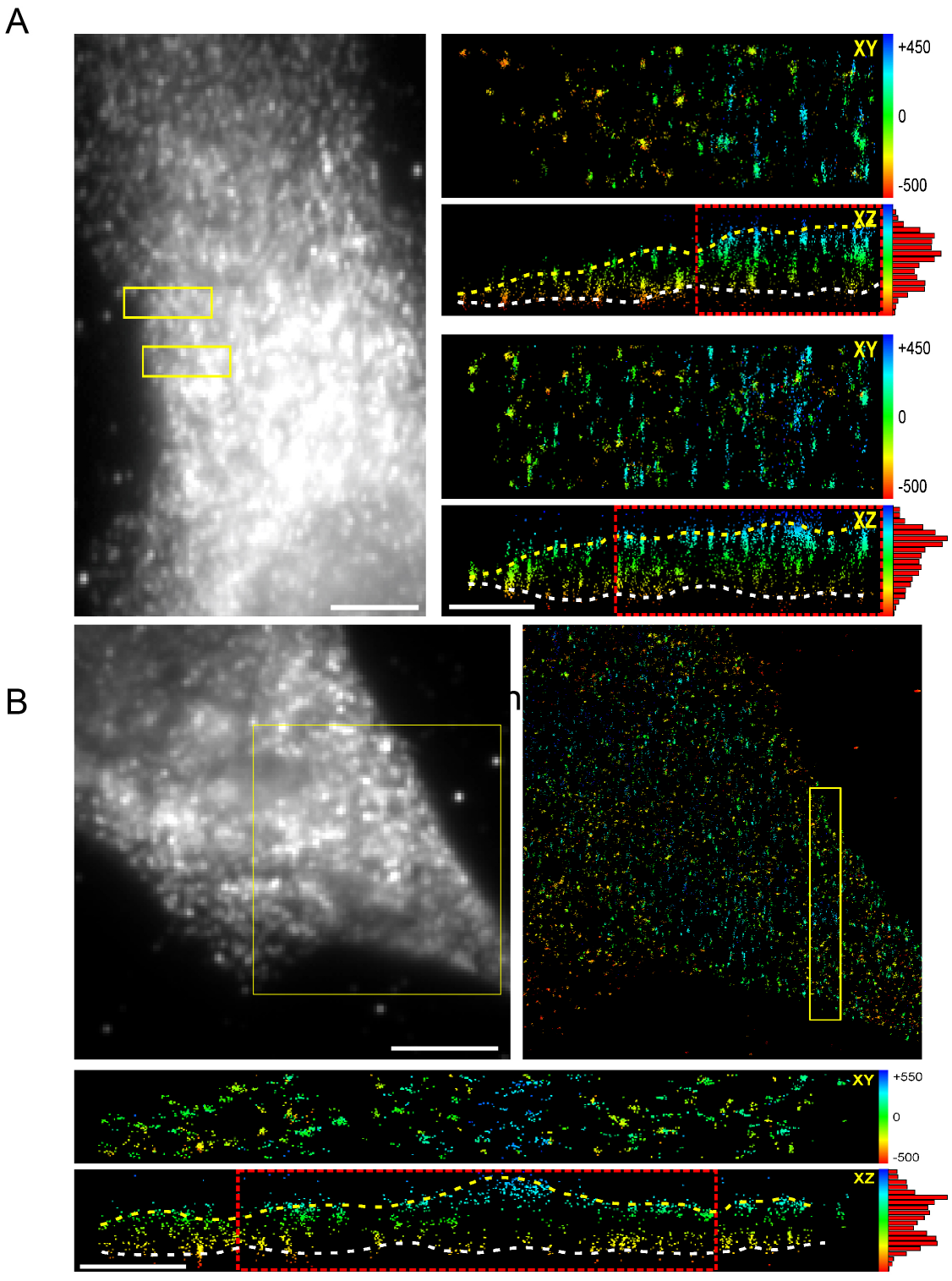

Figure S5 3D dSTORM-imaging of PFA fixed HBMECs.
Alexa-Fluor 647 labeled BACE-1 staining after PFA fixation is shown in two cells **A** and **B**. Diffraction limited image is shown in the overview (left image). BACE-1 is preferentially located close to the plasma membrane as shown by the cross-sections of

small insets (XZ). The yellow and white dotted lines mark the apical (top) and basal (bottom) plasma membranes respectively. Insets are color-coded according to the relative z-position in nm, as indicated by the values. Scale bar 10 and 1μm (overview and insets, respectively). The apico-basal distribution is however different in the two cells indicating a loss of polarization similar to that observed in methanol fixed cells (figure S4A and main figure 4C).